Arc Contraction Behavior of GMA Welding Process Based on Change of Arc Length at Hyperbaric Air Condition

Jiqiang Huang, Wenwen Guo, Junfen Huang, Long Xue, Jizong Wang, and Yong Zou

Abstract   The underwater hyperbaric dry GMA welding method is one of the best emergency maintenance methods for underwater structures. With the increase of ambient pressure, GMA welding quality decreases. The main reason is that GMA welding arc shrinks under high pressure, which leads to the instability of welding process. In order to find out the main factors that affect the contraction of GMA welding arc, theoretical analysis, numerical simulation and experimental verification are used to study the contraction behavior of GMAW arc under high pressure. Based on the governing equation of high-pressure GMA welding arc, the numerical simulations of GMA welding arc under the two conditions of constant arc length and arc length adjustment were carried out by FLUENT software under the environmental pressure of 0.1 MPa, 0.3 MPa, 0.5 MPa and 0.7 MPa, respectively. The contraction of the arc under the two arc length conditions was compared. Through the underwater high-pressure GMA welding test platform, the welding experiments under 0.1, 0.3, 0.5 and 0.7 MPa ambient pressures were carried out. A high-speed camera was used to obtain the arc morphology under different ambient pressures. It was verified the accordance between the experiment results and the simulation data. The results show that the axial and radial dimensions of hyperbaric GMA welding arc decrease with the increase of ambient pressure, showing the phenomenon of arc contraction, especially the arc length decreases significantly, which increases the frequency of short-circuit drop transfer and affects the stability of welding process.

Keywords Hyperbaric welding · Underwater welding · Gas metal arc welding · Arc contraction · Arc self-adjustment · Numerical simulation

J. Huang · W. Guo · J. Huang (✉) · L. Xue · J. Wang · Y. Zou
Beijing Institute of Petrochemical Technology, Beijing 102617, China
e-mail: huangjunfen@bipt.edu.cn

1 Preface

With the rapid development of exploitation and utilization of marine resources, underwater welding technology as an effective method for installation and emergency repair of underwater structures has attracted wide attention. Among the numerous underwater welding methods, the underwater high-pressure dry welding method has become a research hotspot at home and abroad due to its characteristics of good welding quality and high safety [1–3]. Underwater high-pressure dry welding method is conducted in the high-pressure chamber, where the environmental pressure increases as water depth increases, which would lead to welding arc contraction and instability of welding process. The impacts are greater in GMAW; it affects the welding droplet transition and even the whole welding process when the welding parameter adjustment is improper, which seriously deteriorates the underwater welding quality.

Scholars at home and abroad have done a lot of research on the stability and welding quality of high-pressure welding. In the early stage, Perlman did a lot of research on the influence of high-pressure environment on GMAW welding, but the research was not in-depth enough due to the limited research means at that time [4]. Azsar et al. used statistical methods to predict the behavior and stability of GMAW welding arc and proposed that the mismatch of welding current and voltage would have a great impact on the stability of welding process in high-pressure environment [5]. Hart et al. studied the influence of high-pressure GMAW dynamic electrical characteristics and the impact on weld penetration and weld width of environmental pressure, providing reference for quality control of high-pressure welding forming [6]. Akselsen et al. studied the weld performance of X70 pipeline steel under high pressure [7], and Akselsen et al. studied the welding performance of duplex stainless steel under high pressure [8]. The research team of the author studied the weld forming and properties obtained by different welding processes under high-pressure environment [9–11]. Most of the above researches focus on obtaining welding seams of higher quality by various means under high-pressure environment. There are few researches on arc shrinkage causes and shrinkage behaviors under high-pressure environment, failing to reveal the adverse effects of high-pressure environment on the welding process fundamentally.

Jiang et al. studied the high-pressure GTAW arc, revealing the characteristics of the high-pressure GTAW arc, which increased with the increase of environmental pressure [12]. The author studied the characteristics of high-pressure GMAW arc and found that the arc voltage of high-pressure GMAW increased as environmental pressure increases [13]. Li et al. also studied the behavior of high-pressure GMAW welding arc, and again verified that the electric field intensity in the arc column increases with the increase of environmental pressure [14]. These studies have explored the arc behavior in high-pressure environments, but the arc shrinkage behavior mechanism has not been explained systematically.

In this paper, in terms of the high-pressure GMAW welding process, the shrinkage behavior of high-pressure GMAW arc is preliminarily studied by numerical simulation and experimental methods, considering the self-regulating effect of arc, so as to reveal the internal mechanism of arc shrinkage of high-pressure GMAW and provide basic data for the solution of unstable problem in high-pressure welding process.

2 Governing Equation of High-Pressure GMAW Welding Arc

GMAW welding arc can be regarded as the local thermal dynamic equilibrium (LTE) state. It is considered that the plasma of welding arc is optically thin, where the radiation re-absorption in the arc region is so small compared with the total radiation loss that it is ignored. The arc is mapped to the cylindrical coordinate system, and the governing equation of the high-pressure GMAW welding arc is expressed as follows.

When the arc is in a dynamic stable process, the mass of the fluid flowing in and out of the arc region is zero, thus the mass continuity equation is:

$$\frac{1}{r}\frac{\partial}{\partial r}(r\rho v_r) + \frac{\partial}{\partial z}(\rho v_z) = 0 \tag{1}$$

where r is the radial distance between the calculation unit and the welding wire axis, z is the axial distance between the calculation unit and the welding wire end, ρ is the density, v_r, v_z is the radial velocity component and the axial velocity component, respectively.

The energy conservation equation is

$$\frac{1}{r}\frac{\partial}{\partial r}(r\rho v_r h) + \frac{\partial}{\partial z}(\rho v_z h) = \frac{1}{r}\frac{\partial}{\partial r}\left(r\frac{\lambda}{c_p}\frac{\partial h}{\partial r}\right) + \frac{\partial}{\partial z}\left(\frac{\lambda}{c_p}\frac{\partial h}{\partial z}\right)$$
$$+ \frac{5k_b}{2e}\left(\frac{j_r}{c_p}\frac{\partial h}{\partial r} + \frac{j_z}{c_p}\frac{\partial h}{\partial z}\right) + \frac{j_r^2 + j_z^2}{\sigma} - S_r \tag{2}$$

where h is the specific enthalpy, λ is the thermal conductivity, j is the current density, c_p is the specific heat, and S_r is the radiant heat loss, which can be calculated by Stefan-Boltzmann empirical correction formula:

$$S_r = \varepsilon A \zeta T^4$$

where ε is the emissivity of the object, A is the radiation area, and T is the thermodynamic temperature of the blackbody and ζ is constant 5.67×10^{-8} W/(m^2 K^4).

The radial and axial momentum equations are shown in Eqs. (3) and (4), respectively.

$$\frac{1}{r}\frac{\partial}{\partial r}\left(r\rho v_r^2\right) + \frac{\partial}{\partial z}(rv_r v_z) = -\frac{\partial p}{\partial r} + \frac{1}{r}\frac{\partial}{\partial r}\left(2r\mu\frac{\partial v_r}{\partial r}\right)$$
$$+ \frac{\partial}{\partial z}\left(\mu\frac{\partial v_r}{\partial z} + \mu\frac{\partial v_z}{\partial r}\right) - \frac{2\mu v_r}{r^2} - j_z B_\theta \quad (3)$$

$$\frac{1}{r}\frac{\partial}{\partial r}(r\rho v_z v_r) + \frac{\partial}{\partial z}\left(\rho v_z^2\right) = -\frac{\partial p}{\partial z} + \frac{\partial}{\partial z}\left(2\mu\frac{\partial v_z}{\partial z}\right)$$
$$+ \frac{1}{r}\frac{\partial}{\partial r}\left(\mu r\frac{\partial v_z}{\partial r} + \mu r\frac{\partial v_r}{\partial z}\right) + j_r B_\theta + \rho g \quad (4)$$

where μ is the viscosity, and j_r, j_z is the radial and axial current density components, respectively, B_θ is the magnetic field strength and is the pressure.

Current continuity equation:

$$\frac{1}{r}\frac{\partial}{\partial r}\left(r\sigma\frac{\partial \phi}{\partial r}\right) + \frac{\partial}{\partial z}\left(\sigma\frac{\partial \phi}{\partial z}\right) = 0 \quad (5)$$

Ohm's law:

$$j_r = -\sigma\frac{\partial \phi}{\partial r}, \quad j_z = -\sigma\frac{\partial \phi}{\partial z} \quad (6)$$

The magnetic field intensity is given by Maxwell's equation

$$B_\theta = \frac{\mu_0}{r}\int_0^r j_z r\,\mathrm{d}r \quad (7)$$

In Eqs. (5), (6), and (7), ϕ is the electric potential, μ_0 is the permeability, and σ is the conductivity.

3 Numerical Simulation of High-Pressure GMAW Arc with Fixed Arc Length

For the numerical simulation of high-pressure GMAW welding arc, some hypothesis is put forward: (1) The welding arc burns stably with internal heat transfer, and the arc is in an incompressible state of laminar flow; (2) the arc is steady-state and axisymmetric, and the arc model can be simplified into a two-dimensional model; (3) the welding base material is a plane, which means the influence of molten pool and molten drop on the arc shape is ignored.

FLUENT software was used in numerical simulation of welding arc. The simulated welding arc area was the ABCD square area as shown in Fig. 1, with a horizontal length of 14 mm and a vertical length of 16 mm. According to the above assumptions,

Fig. 1 Numerical
simulation area
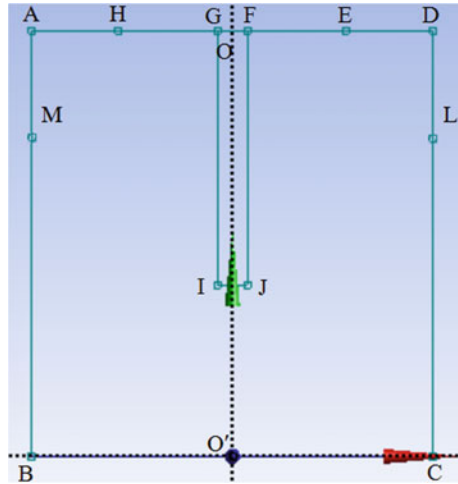
the welding arc area is symmetric about the center axis OO′. AH, ED is the welding protection gas inlet; EF, GH is the end edge of the conductive nozzle; GIJF is the edge of the extension part of the welding wire; the diameter of the wire IJ is 1.2 mm; M, L is the lower end of the nozzle; BC is the base material surface; and the arc area is between IJ and BC.

The boundary conditions defined are shown in Table 1, where v_g is the airflow inlet velocity, v_w is the wire feeding velocity, and the physical parameters of the arc refer to the physical parameters of argon at different temperatures [15].

In the numerical model above, the environmental pressure of GMAW welding is set as 0.1, 0.3, 0.5, 0.7 MPa and the welding current is 250 A. The result is shown in Fig. 2; as can be seen from the diagram, with the increase of the environmental pressure, the bright area of the arc gradually becomes thinner and thinner, which shows that the arc tends to decrease in the radial direction when pressure increases.

In order to further observe and compare the high-temperature area of the arc, the high-temperature area is highlighted by adjusting the numerical simulation result

Table 1 Boundary conditions

Boundary	u	v	φ	T/K
OO′	$\frac{\partial u}{\partial r} = 0$	0	$\frac{\partial \phi}{\partial z} = 0$	$\frac{\partial T}{\partial r} = 0$
O′C	0	0	0	1600
CD	$\frac{\partial u}{\partial r} = 0$	0	$\frac{\partial \phi}{\partial z} = 0$	1000
DE	0	v_g	$\frac{\partial \phi}{\partial z} = 0$	298
EF	0	0	$\frac{\partial \phi}{\partial z} = 0$	1000
FO	0	v_w	$-\sigma \frac{\partial \varphi}{\partial r} = \frac{1}{\pi R^2}$	298

(a) 0.1MPa   (b) 0.3MPa

(c) 0.5MPa   (d) 0.7MP
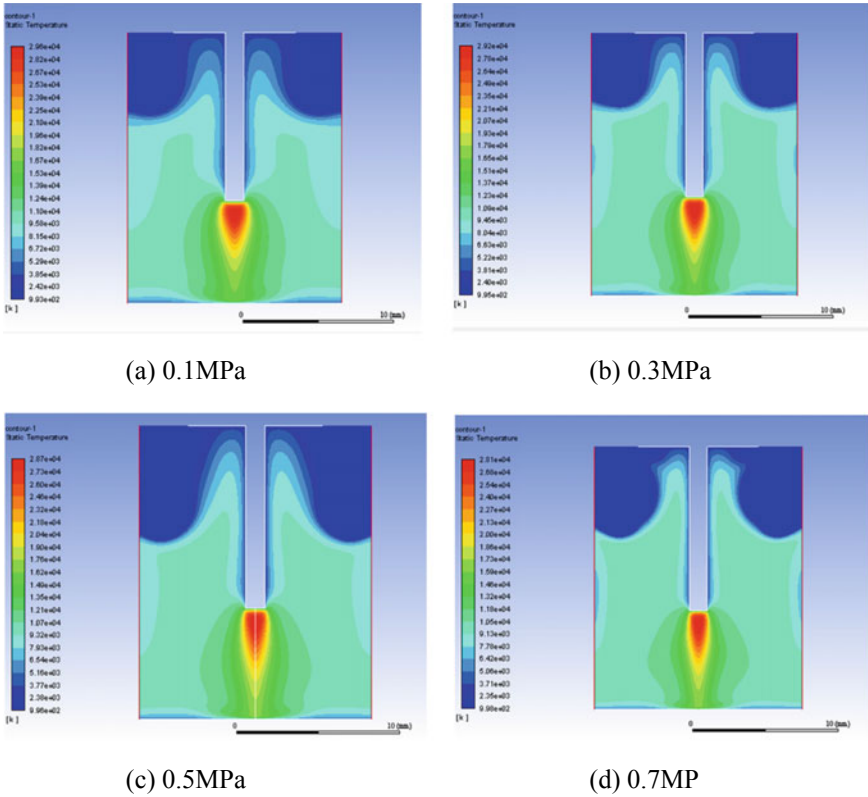
Fig. 2 Simulation results of arc in different ambient pressure/welding current 250 A

ruler to 0–12,000 K, where the temperature higher than 12,000 K is white, as shown in Fig. 3. From the center of the high-temperature area, it is obvious that, with the increase of environmental pressure, the high-temperature of arc area decreased
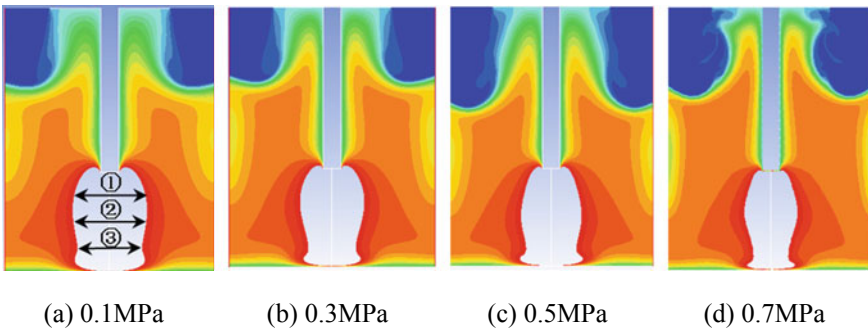

(a) 0.1MPa   (b) 0.3MPa   (c) 0.5MPa   (d) 0.7MPa

Fig. 3 High temperature of arc in different pressures

Table 2 Radial dimension of the arc at different pressures/mm

Position	Pressure/MPa			
	0.1	0.3	0.5	0.7
①	5.2	4.5	4.0	3.3
②	5.0	4.3	4.4	3.8
③	4.5	3.4	3.7	3.0

significantly in the radial direction. In order to further analysis, three locations are chosen in the height direction of the arc, as shown in Fig. 3a. The diameter of the luminous part of the arc was measured as is shown in Table 2. It can be seen that with the increase of the environmental pressure, the arc diameter in the high-temperature area of the arc decreases significantly, the shape of the arc changes from a bell jar to a bowling ball, and the arc shrinks more obviously in the anode area.

4 Numerical Simulation of High-Pressure GMAW Arc with Arc Length Adjustment

## 4.1 Arc Length Variation Under High-Pressure Environment

In the actual GMAW welding process, due to the self-regulating effect of arc length, it will be automatically adjusted to the appropriate length as the environment changes to meet the requirements of the minimum voltage principle [16]. In the high-pressure environment, due to the change of heat dissipation conditions in the ambient atmosphere, the dissipated energy of the welding arc increases, resulting in the increase of electric field intensity E of the welding arc [12–14]. Under the condition that the output voltage U of the welding power supply remains unchanged, the changes of arc length la of the arc are discussed as follows.

GMAW welding circuit is shown in Fig. 4. The output voltage of welding power supply is U, the equivalent output inductance and resistance in the circuit are denoted as L and R, respectively, and the voltage drop on it is U_L and U_R, respectively. The extension length of welding wire is l_s, the voltage drop of welding wire is U_s, and the voltage drop of arc is U_a; then there is

$$U = U_R + U_L + U_\mathrm{s} + U_\mathrm{a} \qquad (8)$$

In the formula, $U_R = I R$, $U_L = L\frac{\mathrm{d}I}{\mathrm{d}t}$, $U_\mathrm{s} = \rho\frac{l_\mathrm{s}}{s}I$, $U_\mathrm{a} = El_\mathrm{a}$ where I is the current flowing in the circuit. During the stable GMAW welding process, the welding current does not change much, so the voltage drop on the inductance can be approximately 0. ρ is the wire resistivity; s the cross-sectional area of the welding wire, and for the convenience of discussion, Formula (8) can be written as

Fig. 4 Welding circuit schematic
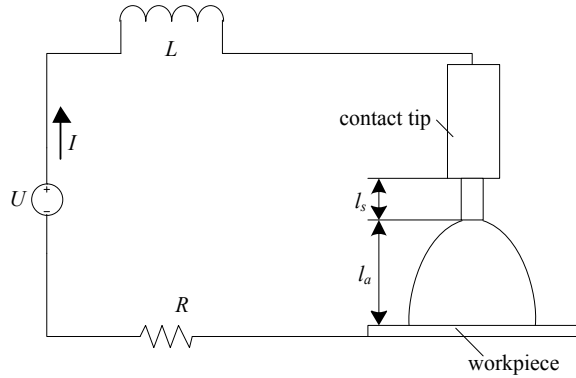
$$U = K + l_\mathrm{a}\left(E - \frac{\rho}{s}I\right) \tag{9}$$

In terms of $K = RI + \rho\frac{l_s + l_a}{s}I$, In the stable welding process, K is basically unchanged. It can be seen from the above equation that under the high-pressure environment, electric field intensity E increases, and under the condition that the output voltage of welding power remains unchanged, arc length l_a decreases as the environmental pressure increases; that is, the arc shrinks in the axial direction.

4.2 Simulation Results of High-Pressure GMAW with Arc Length Variation

On the basis of the high-pressure GMAW welding arc change analysis above, considering the GMAW welding arc axial size changes, correction of the welding arc model is conducted with the environmental pressure of 0.3, 0.5, 0.7 MPa, and the welding current of 250 A, taking the information of arc length changes into the simulation model, as the reference Formula (9). The numerical simulation results are shown in Fig. 5. According to the aforementioned ruler adjustment method, the high-temperature region is highlighted and compared with the simulation results under atmospheric pressure, as shown in Fig. 6. High-temperature area axial and radial dimension measuring position is as shown in Fig. 6a and b, and the results of the measurement are shown in Table 3; it can be seen that with the increase of environmental pressure, electric arc of high-temperature area of the axial and radial dimensions shows a decrease trend, which means that with the increase of environmental pressures, arc contraction appears.
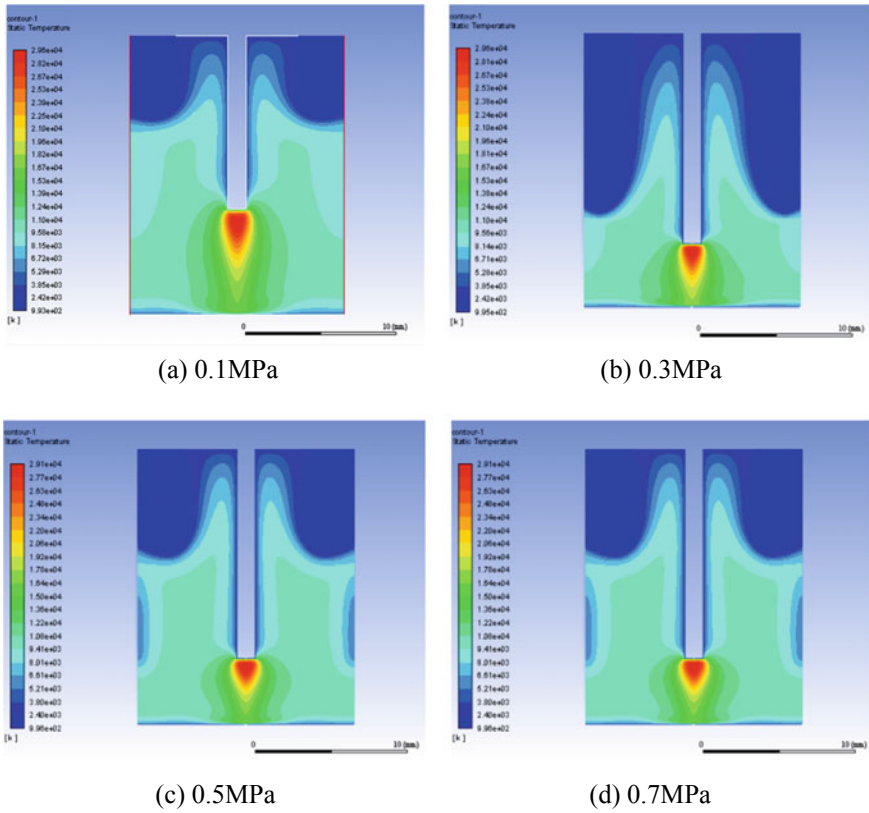
(a) 0.1MPa

(b) 0.3MPa

(c) 0.5MPa

(d) 0.7MPa

Fig. 5 Numerical simulation results considering the change of arc length

(a) 0.1MPa   (b) 0.3MPa   (c) 0.5MPa   (d) 0.7MPa
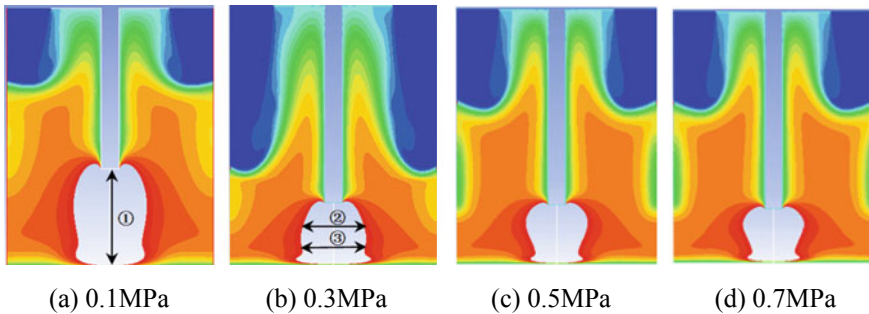
Fig. 6 Measuring position

Table 3 Numerical simulation of arc radial dimension

Position	Pressure/MPa			
	0.1	0.3	0.5	0.7
①	7.8	4.8	4.4	4.1
②	5.4	5.2	5.2	4.8
③	5.3	5.0	3.5	3.9

5 Experimental Results and Discussion

With the help of the high-pressure welding test platform (as shown in Fig. 7), the high-pressure GMAW welding test and arc morphology observation are conducted. The high-pressure welding test platform includes the high-pressure test chamber, air compression system, monitoring and control system, welding system and image acquisition system, etc. The block diagram is shown in Fig. 8. The welding power supply is Fronius CMT3200, the image acquisition USES MS55K color digital high-speed camera. Parent metal is made of Q235 steel plate, wire type ER50-6, wire diameter is 1.2, 15 mm wire stem elongation, welding current is 250 A, welding voltage 28.2 V, the welding speed is 25 cm, 1 min, welding protective gas is 80% Ar + 20% CO_2 gas mixture, shielding gas flow to 20 l, 1 min, welding environment pressure: 0.1, 0.3, 0.5, and 0.7 MPa, obtain the high-pressure GMAW welding process of arc photographs as shown in Fig. 9.

The luminous area of the arc image is measured as is shown in Fig. 9, including the axial and radial dimensions of the arc. The specific measurement results are shown in Table 4. Through data analysis, it can be found that with the increase of environmental pressure, the axial and radial dimensions of high-pressure GMAW welding arc both decrease, indicating the shrinkage of high-pressure GMAW arc, which is consistent with the previous simulation results. The simulation results and experimental results
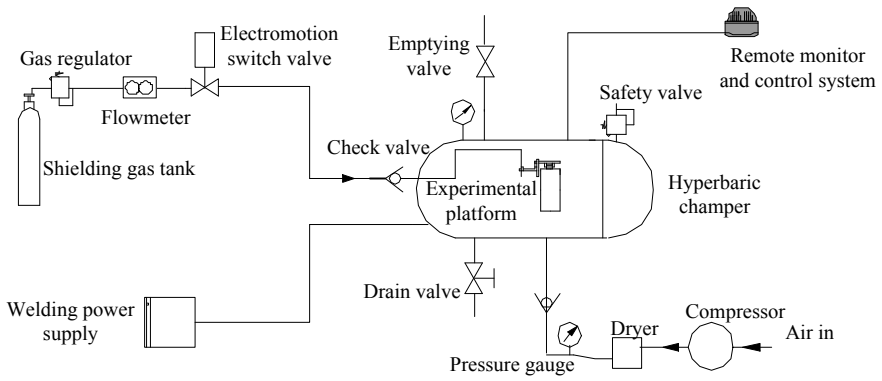
Fig. 7 High-pressure GMA welding equipment
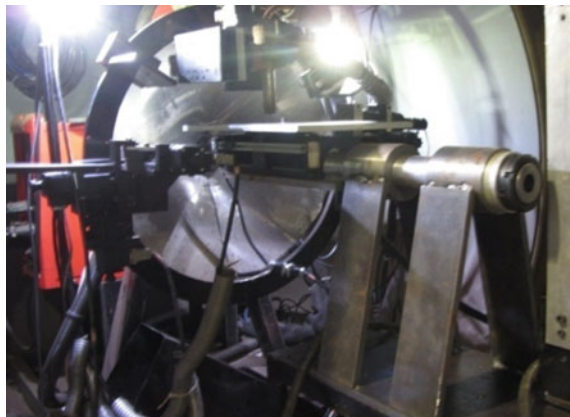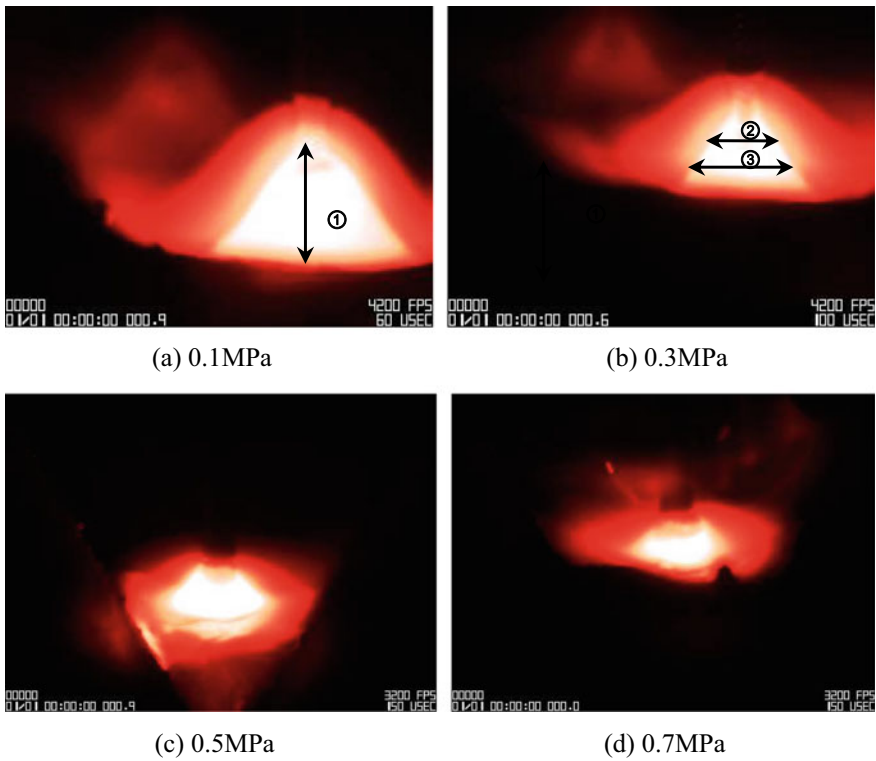
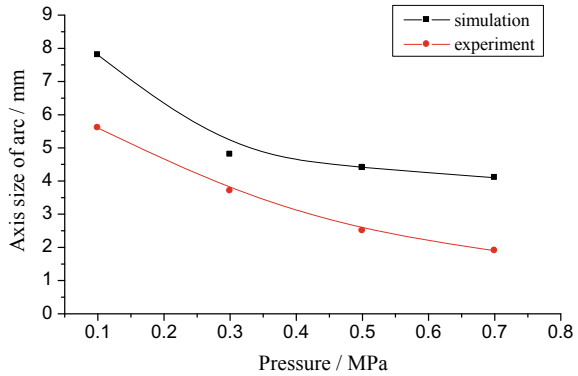**Fig. 8** Schematic diagram of hyperbaric welding equipment

(a) 0.1MPa

(b) 0.3MPa

(c) 0.5MPa

(d) 0.7MPa

Fig. 9 Pictures of welding arc at different pressures

Table 4 Arc sizes of hyperbaric welding with current 250 A

| Position	Pressure/MPa			
	0.1	0.3	0.5	0.7
①/mm	5.6	3.7	2.5	1.9
②/mm	5.1	2.8	2.7	2.5
③/mm	6.7	6.0	4.5	4.1

Fig. 10 Change of arc length with pressure

of the axial dimension of GMAW welding arc are given in Fig. 10. It can be seen clearly that the sizes of the two results tend to decrease with the increase of welding pressure. However, the axial dimensions in the simulation results are higher than the experimental results, because the influence of arc adaptive adjustment factors on the decrease of arc axial dimensions is considered in the simulation process. In fact, there are many factors affecting the decrease of arc axial dimensions, which need to be further explored. According to the experimental and simulation results, the axial dimension (arc length) of the arc decreases significantly in the high-pressure GMAW welding process. If the arc length is too short, it will directly affect the way of droplet transition, resulting in an increase of short-circuit frequency in the welding process and the instability of the arc. Therefore, in the actual high-pressure GMAW welding process, the welding voltage should be appropriately increased according to the increase of the environmental pressure, which is conducive to the welding arc to maintain a proper arc length, to avoid frequent short circuit caused by the arc length is too low, so as to improve the stability of the arc.

Figure 11 shows the high-pressure GMAW welding arc radial size of the simulation and experiment results, both of which decrease as the environment pressure increases. The reduction in simulation results is smaller than in the experimental results. The reasons of the difference may be: (1) the simulation results of the bright area sets 12,000 K (when the degree of ionization of about 0.5%) as the boundary, but the actual welding bright area is slightly different; (2) during the experimental welding, the dynamic change of high-pressure GMAW welding arc is large. The

Fig. 11 Change of arc radial sizes with ambient pressure
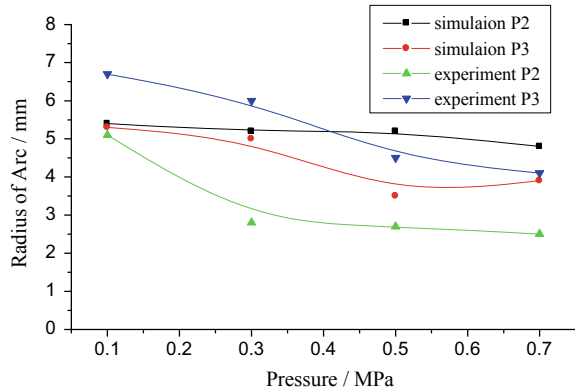
subjects of the study all choose the arc images with the largest luminous area of the burning arc, but there are differences in the morphology of the luminous area, and there are certain differences in the determination of the arc measurement position. But generally speaking, the simulation and experimental results of arc radial dimension have a good agreement, and both reflect the trend that radial dimension decreases with the increase of environmental pressure.

6   Conclusion

On the basis of the high-pressure GMAW welding arc simulation with constant arc length, considering arc length adjustment, the high-pressure GMAW welding arc is simulated, which is compared with experimental results welding test. The results show that axial and radial sizes of high-pressure GMAW welding arc are gradually contracted with the increase of environmental pressure, especially that the arc length is reduced obviously, thus increasing the short-circuit transition frequency and affecting the stability of welding process. In the actual welding process, welding voltage should be appropriately improved.

References

1. Woodward N (2006) Developments in diverless subsea welding. Weld J 10:35–39
2. Richardson IM, Woodward NJ, Armstrong MA, Berge JO (2010) Developments in dry hyperbaric arc welding—a review of progress over the past ten years. In: International workshop on

the state of the art science and reliability of underwater welding and inspection technology, Houston, Texas, USA, pp 65–83

3. Shi Y, Zhang X, Lei Y et al (2000) Advances in welding technology under harsh conditions. J Mech Eng 13–16

4. Azsar AS, Woodward N, Fostervoll H, Akselen O (2012) Statistical analysis of the arc behavior in dry hyperbaric GMA welding from 1 to 250 bar. J Mater Process Technol 212(1):211–219

5. Hart P, Richardson IM, Nixon JH (2001) The effects of pressure on electrical performance and weld bead geometry in high pressure GMA welding. Weld World 45(11/12):29–37

6. Perlman M, Pense AW, Stout RD (1969) Ambient pressure effects on gas metal-arc welding of mild steel. Weld J 6:231–238

7. Akselsen OM, Fostervoll H, Ahlen CH (2009) Hyperbaric GMA welding of duplex stainless steel at 12 and 35 bar. Weld J 88(2):21s–28s

8. Akselsen OM, Fostervoll H, Harsvcer A et al (2006) Mechanical properties in hyperbaric GTA welding of X70 pipeline. In: Proceedings of the sixteenth international offshore and polar engineering conference, San Francisco, California, USA, pp 152–159

9. Huang J, Xue L, Huang J et al (2016) Arc behavior and joints performance of CMT welding process in hyperbaric atmosphere. Acta Metall Sin 52(01):93–99

10. Liu H, Xue L, Huang J et al (2016) Influence of environmental pressure on strength and toughness of weld by gas metal arc welding. J Shanghai Jiao Tong Univ 50(10):1613–1617

11. Huang J, Xue L, Huang J et al (2016) Effects of welding polarity on weld appearance of pulsed GMAW in hyperbaric environments. J Mech Eng 52(18):64–69

12. Jiang LP, Wang Z, Jiao X et al (2007) Characteristics of GTAW arc in underwater welding under high-pressure air condition. Trans China Weld Inst 28(6):1–4

13. Jiqiang H, Long X, Tao L et al (2012) Arc characteristics of GMA welding in high-pressure air condition. China Weld 21(4):26–31

14. Li K (2014) Study on GMAW arc behavior and droplet transition by high pressure dry method. Dissertation, Harbin Institute of Technology

15. Fan HG, Kovacevic R (1998) Dynamic analysis of globular metal transfer in gas metal arc welding—a comparison of numerical and experimental results. J Phys D Appl Phys 31(20):2929–2941

16. Yin S (2016) Process foundation and application of gas shielded welding. J Mech Eng 60–61